Bulletin of Earthquake Engineering
https://doi.org/10.1007/s10518-018-0503-9

ORIGINAL RESEARCH

The peak over the design threshold in strong earthquakes

Iunio Iervolino[1] · **Massimiliano Giorgio**[2] · **Pasquale Cito**[1]

Received: 30 April 2018 / Accepted: 17 October 2018

Abstract
In state-of-the-art seismic design, reference seismic actions are based on probabilistic seismic hazard assessment, which provides the ground-motion intensity corresponding to a reference return period of exceedance at the site. Exceedance of elastic actions, which is systematically observed in the epicentral areas of strong earthquakes, does not necessarily mean violation of the structural design limit-state; nevertheless, in such a case, the safety margins inherent to design are left to other factors beyond the elastic spectrum, which are, in general, not explicitly controlled. Therefore, it might be useful to quantify the expected (i.e., mean) amount of ground-motion intensity exceedance in earthquakes for which the design spectrum is not conservative. In fact, this study, with reference to Italy, provides and discusses the map of the expected value of acceleration, given the exceedance of the design spectra at any site in the country. It is shown, among other results, that: (1) the expected exceedance varies significantly from site-to-site across the country despite the same return period of the threshold is considered everywhere, (2) its pattern is opposite to that of the ε from disaggregation, and (3) the peak-over-the-threshold can be larger than 2.5 times than the corresponding ordinate of the design spectrum with 475 years return period. These results may be informative about what to expect for code-conforming structures in terms of seismic actions during strong earthquakes, that is, those able to cause exceedance of design elastic spectra.

Keywords Performance-based seismic design · Building code · Seismic structural safety

1 Introduction

When design seismic actions are based on probabilistic seismic hazard analysis (PSHA) (e.g., McGuire 2004), they are usually in the form of uniform hazard spectra (UHS'); i.e., spectra with ordinates that have the same rate, or equivalently, the same return period of exceedance $\left(T_r\right)$. For example, according to the Italian building code (CSLLPP 2008), the *life-safety* limit-state of an ordinary structure, corresponding to *significant-damage* in

✉ Iunio Iervolino
iunio.iervolino@unina.it

[1] Dipartimento di Strutture per l'Ingegneria e l'Architettura, Università degli Studi di Napoli Federico II, Naples, Italy

[2] Dipartimento di Ingegneria, Università degli Studi della Campania Luigi Vanvitelli, Aversa, Italy

Published online: 22 October 2018

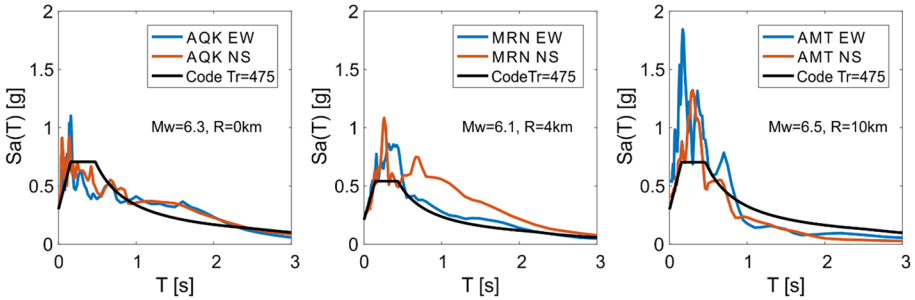

Fig. 1 Comparison of recorded and code spectra at three seismic stations: AQK (*L'Aquila downtown*) during L'Aquila (2009) earthquake (left), MRN (*Mirandola*) during the Emilia (2012) earthquake (center), and AMT (*Amatrice*) during the central Italy (2016) earthquake (right). Design spectra are adjusted for the site conditions reported in the Italian Accelerometric Archive (http://itaca.mi.ingv.it/)

Eurocode 8 (CEN 2004), must be verified against the spectrum the ordinates of which are exceeded at the site, on average, every 475 years.

Nowadays, the continuously extending seismic monitoring networks provide an unprecedented amount of data that allows a thorough comparison of design spectra with the counterparts recorded in earthquakes.[1] Such a comparison shows that design spectra are often largely exceeded in the near-source area of events whose magnitudes are relatively far from the maximum deemed possible in hazard assessment. As an example, Fig. 1 shows the spectra recorded at some seismic stations during the mainshocks of the latest three most relevant seismic sequences that occurred in Italy: L'Aquila 2009 (Masi et al. 2011), Emilia 2012 (Chioccarelli et al. 2012) and central Italy 2016 (Iervolino et al. 2017a). The considered earthquakes had moment magnitude, Mw, equal to 6.3, 6.1 and 6.5, respectively (according to the Italian parametric earthquake catalog; https://emidius.mi.ingv.it/CPTI/). In particular, the figure shows the Italian code spectra for $T_r = 475$ years for the sites where also a seismic station was present at the time of the earthquake. All the stations are somewhat close to the source (R is the source-to-site distance in terms of *Joyner & Boore* metric; Joyner and Boore 1981) and it can be observed that the design spectra have been exceeded in wide ranges of periods and by a large amount.

It has been extensively discussed, with reference to these same events, that such observations do not contradict but rather confirm PSHA, as the exceedance of hazard-based design spectra is well expected at sites near the source of moderate-to-high earthquakes; e.g., Iervolino et al. (2017a), Iervolino and Giorgio (2017). In other words, seismic design actions from PSHA, are likely (inherently) not conservative in a region around the source the size of which depends on the magnitude. The structural engineering consequence of this well-known issue is that, in these areas, structures must withstand elastic actions beyond elastic spectra and, to date, in this case their behavior is not explicitly controlled, even by state-of-the-art seismic codes (Iervolino et al. 2017b).

The simple study presented herein intends to further deepen this issue, providing quantitative insights with reference to Italy. In particular, using the same source model adopted to develop the hazard at the basis of the current code, the map of the amount of exceedance,

[1] The caveats of such a comparison, which is less trivial than it can appear, have been discussed by a number of authors; e.g., Iervolino (2013), Barani et al. (2017a, b).

namely the *peak-over-the-threshold*, is provided and discussed. In fact, it is the expected acceleration given exceedance of the design threshold, which is related to the action a structure should undergo during strong earthquakes (Iervolino et al. 2018).

The discussion mainly refers to two spectral ordinates, in terms of pseudo-acceleration, with 475 years return period of exceedance. Two sites in the country, exposed to low- and high-hazard, are also used to extend the discussion to a range of return periods of design interest.

2 Italian probabilistic seismic hazard model

In this section, before introducing the models employed to assess seismic hazard in Italy, the essentials of PSHA and hazard disaggregation are recalled. The framing equation of single-site PSHA is Eq. (1); it provides, for a (pseudo) spectral acceleration (Sa), referring to a given natural vibration period (T) and damping factor, the (annual) rate, λ, of earthquakes exceeding any arbitrary threshold (sa).

$$\lambda_{Sa(T)>sa} = \sum_{i=1}^{s} \nu_i \cdot \iint_{M,R} P[Sa(T) > sa | M = m, R = r] \cdot f_{M,R,i}(m, r) \cdot dr \cdot dm \tag{1}$$

In the equation, $\nu_i, i = \{1, 2, \ldots, s\}$, is the rate of earthquakes above a minimum magnitude of interest and below the maximum magnitude deemed possible for each of the s seismic sources affecting the site. The term $f_{M,R,i}(m, r)$ is the joint probability density function (PDF) of magnitude (M) and source-to-site distance (R) for the ith source, and $P[Sa(T) > sa | M = m, R = r]$ is the probability of exceeding the sa threshold conditional to $\{M, R\}$, provided by a ground-motion prediction equation (GMPE). (The GMPE considered can also vary with the seismic source zone; however, this dependency is neglected herein to simplify the notation.)

Computing the hazard integral for a set of different thresholds provides the so-called hazard curve, representing the exceedance rate as a function of sa. Developing hazard curves for a set of spectral ordinates, corresponding to different natural vibration periods yields the UHS for any T_r of interest. These spectra are obtained entering all hazard curves with an exceedance rate equal to the reciprocal of T_r and plotting the corresponding acceleration values, say sa_{T_r}, versus the natural periods.

2.1 Seismic source model and hazard map

The source model considered for Italy is the one by Meletti et al. (2008), which features thirty-six seismic source zones numbered from 901 to 936 (Fig. 2, left) and no background seismicity. It is at the basis of the Italian hazard study described in Stucchi et al. (2011), which provides the UHS' defining engineering structural seismic actions according to the code (i.e., the design spectra in Fig. 1).[2]

[2] To be precise, in NTC, spectra for A-type site class have the four-regions EC8-type (CEN 2004) functional form. However, such a spectral shape is calibrated site-by-site to approximate the UHS as much as possible. Spectra for other site classes are obtained by applying correction factors to the A-type spectra.

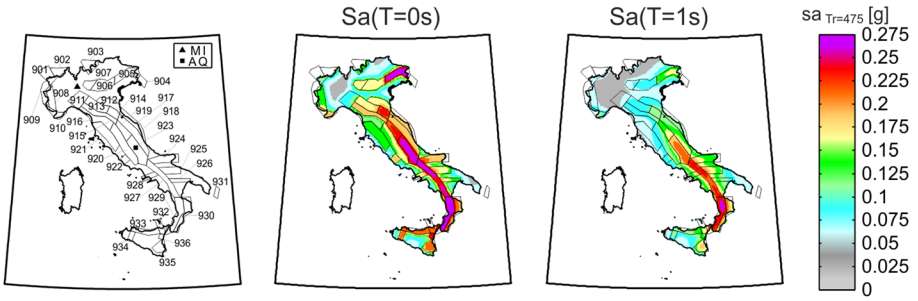

Fig. 2 Left: seismic source zone model for Italy (Meletti et al. 2008); center and right: maps of PGA and 1 s pseudo-spectral-acceleration with 475 years exceedance return period on rock, according to the branch 921 of the logic tree described in Stucchi et al. (2011)

The seismic hazard study described in Stucchi et al. (2011) features a fairly-complex logic tree; herein, the branch named 921 (not to be confused with one of the zones) is considered; it is the one producing the hazard results believed close to those of the full logic tree, which are expressed in the form of so-called *median hazard* (Barani et al. 2009). Branch 921 considers the mentioned zones and the ground-motion prediction equation of Ambraseys et al. (1996). In the calculations, the epicentral location is uniformly-distributed over each source zone, and it is assumed that the hazard for a site is only affected by the events that are less than 230 km away. Epicentral distance is converted into the metric required by the GMPE, the Joyner & Boore distance, using the approach of Montaldo et al. (2005). The style-of-faulting correction factors proposed by Bommer et al. (2003) are also applied to the GMPE, consistent with the rupture mechanism associated with each zone by Meletti et al. (2008). The rates of earthquakes and the magnitude distribution for the zones can be retrieved from Table 1, which provides the rates per surface-wave magnitude bins.[3] The central value of the minimum-magnitude bin considered for the zones is 4.3 (apart from the zone 936 which is the Etna's volcanic area and has a central magnitude of the lowest bin equal to 3.7), while the maximum depends on the zone of interest, but the largest central value of a bin is never above 7.3 (see largest magnitude bin with non-zero rate).[4] Based on this model, Fig. 2 (center and right panels) reports the maps of $Sa(T = 0\text{ s})$, that is the peak ground acceleration (PGA), and $Sa(T = 1\text{ s})$ with 475 years return period of exceedance at any site, considering rock site conditions. To obtain these maps the source zones were discretized via a fine grid with average node spacing of 0.02° or about 2 km. The same grid was also used to discretize the Italian territory in order to define the sites where to compute hazard. The discretization resulted in about eighty-thousand points. The calculations were carried out via the software introduced in Iervolino et al. (2016). It can be seen from the figure that the most hazardous regions are in central and southern Italy, along the Apennines mountain chain. The largest acceleration values with 475 years return period of exceedance are below 0.3 g for both spectral ordinates. The lowest hazard levels occur, as expected, outside the source zones.

[3] Personal communication by Carlo Meletti, *Istituto Nazionale di Geofisica e Vulcanologia*, Pisa, Italy.

[4] According to Table 1, earthquakes of magnitude larger than 6 have rate 0.12 all over the country, which means a return period of 8.6 years. Thus, the systematic (i.e., relatively frequent) exceedance in earthquakes of the kind in Fig. 1 does not justify surprise or a discussion to question the soundness of PSHA used to determine design spectra (see Iervolino and Giorgio 2017, and Iervolino et al. 2018, for demonstration).

Table 1 Annual magnitude rates for the source model of Fig. 2 (left)

	Magnitude ± 0.15												
	3.7	4.0	4.3	4.6	4.9	5.2	5.5	5.8	6.1	6.4	6.7	7	7.3
901	0	0	0.0153	0.0076	0.0166	0.0033	0.0021	0.0021	0	0	0	0	0
902	0	0	0.0534	0.0153	0.0166	0.0099	0	0.0064	0.0014	0	0	0	0
903	0	0	0.0992	0.0076	0.0099	0	0	0.0021	0	0	0	0	0
904	0	0	0.0305	0.0153	0	0	0.0042	0	0	0	0	0	0
905	0	0	0.1687	0.0904	0.0254	0.0106	0.0085	0.0071	0	0.0033	0.0022	0	0
906	0	0	0.0663	0.0482	0.0127	0.0021	0.0042	0	0	0.0011	0	0	0
907	0	0	0.0302	0.0301	0.0021	0	0.0021	0.0014	0	0	0	0	0
908	0	0	0.1069	0.0076	0.0166	0.0066	0.0021	0	0	0	0	0	0
909	0	0	0.0305	0.0076	0.0099	0.0066	0.0021	0	0	0	0	0	0
910	0	0	0.0611	0.0076	0	0.0066	0.0021	0.0064	0	0.0014	0	0	0
911	0	0	0.0305	0.0076	0.0099	0	0.0021	0	0	0	0	0	0
912	0	0	0.0482	0.0120	0.0106	0.0148	0.0021	0.0028	0.0012	0	0	0	0
913	0	0	0.1145	0.0602	0.0169	0.0042	0.0085	0.0014	0	0	0	0	0
914	0	0	0.0843	0.0663	0.0148	0.0085	0.0021	0.0057	0.0014	0	0	0	0
915	0	0	0.1832	0.0763	0.0398	0	0.0042	0.0042	0.0014	0.0014	0	0	0
916	0	0	0.0458	0.0305	0.0085	0.0042	0.0021	0	0	0	0	0	0
917	0	0	0.0542	0.0301	0.0114	0.0085	0.0106	0.0064	0.0012	0	0	0	0
918	0	0	0.1527	0.0229	0.0170	0.0057	0.0085	0.0064	0.0042	0.0014	0	0	0
919	0	0	0.1298	0.0534	0.0297	0.0106	0.0042	0.0071	0.0043	0.0025	0	0	0
920	0	0	0.1832	0.0687	0.0568	0.0085	0	0	0	0	0	0	0
921	0	0	0.1756	0.0840	0.0254	0.0085	0.0021	0.0028	0	0	0	0	0
922	0	0	0.0458	0.0229	0.0169	0.0042	0	0	0	0	0	0	0
923	0	0	0.4122	0.0992	0.0767	0.0227	0.0085	0.0106	0.0021	0.0057	0.0043	0.0014	0.0014
924	0	0	0.0687	0.0382	0.0372	0.0279	0.0140	0	0.0042	0	0.0017	0	0
925	0	0	0.0458	0.0153	0.0047	0	0	0	0	0.0033	0.0017	0	0

Table 1 (continued)

	Magnitude ± 0.15												
	3.7	4.0	4.3	4.6	4.9	5.2	5.5	5.8	6.1	6.4	6.7	7	7.3
926	0	0	0.0305	0.0076	0.0186	0	0.0047	0	0	0	0	0	0
927	0	0	0.2150	0.0561	0.0512	0.0093	0.0047	0.0064	0.0021	0.0042	0.0066	0.0066	0
928	0	0	0.0154	0.0153	0.0186	0	0.0042	0.0021	0	0	0	0	0
929	0	0	0.2243	0.0374	0.0651	0.0186	0.0140	0.0140	0.0085	0.0021	0.0017	0.0066	0.0017
930	0	0	0.1028	0.0093	0.0047	0.0093	0.0093	0.0047	0.0021	0.0021	0.0017	0	0
931	0	0	0.0193	0.0192	0	0	0.0047	0	0	0	0	0.0021	0
932	0	0	0.0748	0.0187	0.0166	0.0033	0	0	0.0042	0	0	0	0
933	0	0	0.1145	0.0153	0.0132	0.0199	0.0066	0.0021	0.0021	0	0	0	0
934	0	0	0.0280	0.0001	0.0099	0.0033	0	0	0.0021	0	0	0	0
935	0	0	0.0534	0.0001	0.0166	0.0099	0.0042	0	0.0021	0	0.0023	0	0.0012
936	0.3359	0.0458	0.0382	0.0153	0.0132	0.0033	0	0	0	0	0	0	0

To introduce the results given in the following, it is useful to explore some details on the seismic hazard assessment for some specific sites in Italy: L'Aquila and Milan (see Fig. 2, left, for their location). They are chosen to represent high- and low-hazard sites, respectively; indeed, the PGA values from Fig. 2 (center) are 0.25 g and 0.05 g, for L'Aquila and Milan, respectively. The corresponding $Sa(T = 1\text{ s})$ values from Fig. 2 (right) are 0.21 g and 0.04 g, respectively.

2.2 Disaggregation

Hazard disaggregation is the procedure, within the PSHA framework, used to determine the earthquake scenarios that most likely cause the exceedance of sa. Before recalling the disaggregation equation, it may be worthwhile to rewrite the hazard integral in the format of Eq. (2) (Bazzurro and Cornell 1999).

$$\lambda_{Sa(T)>sa} = \sum_{i=1}^{s} \nu_i \cdot \iiint_{M,R,\varepsilon} I[Sa(T) > sa | M = m, R = r, \varepsilon = z] \cdot f_{M,R,\varepsilon,i}(m, r, z) \cdot dz \cdot dr \cdot dm \tag{2}$$

In the equation, $f_{M,R,\varepsilon,i}$ is the joint distribution of $\{M, R, \varepsilon\}$, where ε is the standardized residual of a ground-motion prediction equation (a generic realization of ε is indicated as z hereafter). In many cases, it can be written as $f_{M,R,\varepsilon,i}(m, r, z) = f_{M,R,i}(m, r) \cdot f_{\varepsilon}(z)$; in fact, in classical GMPEs (see Douglas 2014) the relationship between sa and the random variables characterizing the seismic sources is of the type in Eq. (3), where $\mu_{m,r}$ is a term depending on $\{M, R\}$, θ represents one or more coefficients accounting, for example, for soil class, and $\sigma \cdot \varepsilon$ is a zero mean and σ^2 variance Gaussian random variable independent of $\{M, R\}$ and of θ.

$$\log(sa) = \mu_{m,r} + \theta + \sigma \cdot \varepsilon \tag{3}$$

Once $\{M, R, \varepsilon\}$ are specified, $P[Sa(T) > sa | M = m, R = r, \varepsilon = z]$ degenerates in the indicator function appearing in Eq. (2), $I[Sa(T) > sa | M = m, R = r, \varepsilon = z]$, that equals one in the case of exceedance of sa and zero otherwise.

At this point Eq. (4) can be introduced, it is the equation framing hazard disaggregation and provides the PDF of $\{M, R, \varepsilon\}$ given the occurrence of a ground-motion such that $Sa(T) > sa$.

$$f_{M,R,\varepsilon|Sa(T)>sa}(m, r, z) = \frac{\sum_{i=1}^{s} \nu_i \cdot I[Sa(T) > sa | M = m, R = r, \varepsilon = z] \cdot f_{M,R,\varepsilon,i}(m, r, z)}{\lambda_{Sa(T)>sa}} \tag{4}$$

The maps of mean $\{M, R, \varepsilon\}$ given the exceedance of $sa_{T_r=475}$ are given in Fig. 3 (disaggregation, and therefore also these maps are independent of subsoil conditions of the sites, that is θ, as demonstrated in Iervolino 2016).

Although the reader should refer to Barani et al. (2009) and Iervolino et al. (2011), where disaggregation for Italy is discussed in larger detail, one notices well-known results for $\{\overline{M}, \overline{R}, \overline{\varepsilon}\}$. In fact, as it regards the mean magnitude (i.e., the expected value of magnitude causing exceedance) it is, generally, relatively far from the maximum of the earthquakes the site can experience (see Table 1), even if it is larger for $Sa(T = 1\text{ s})$ than $Sa(T = 0\text{ s})$. As it regards the distance, for sites enclosed in source zones, the earthquakes most likely causative for the exceedance are, in general, close to the site, even if this distance is, again, larger for $Sa(T = 1\text{ s})$ than $Sa(T = 0\text{ s})$. Clearly, the mean

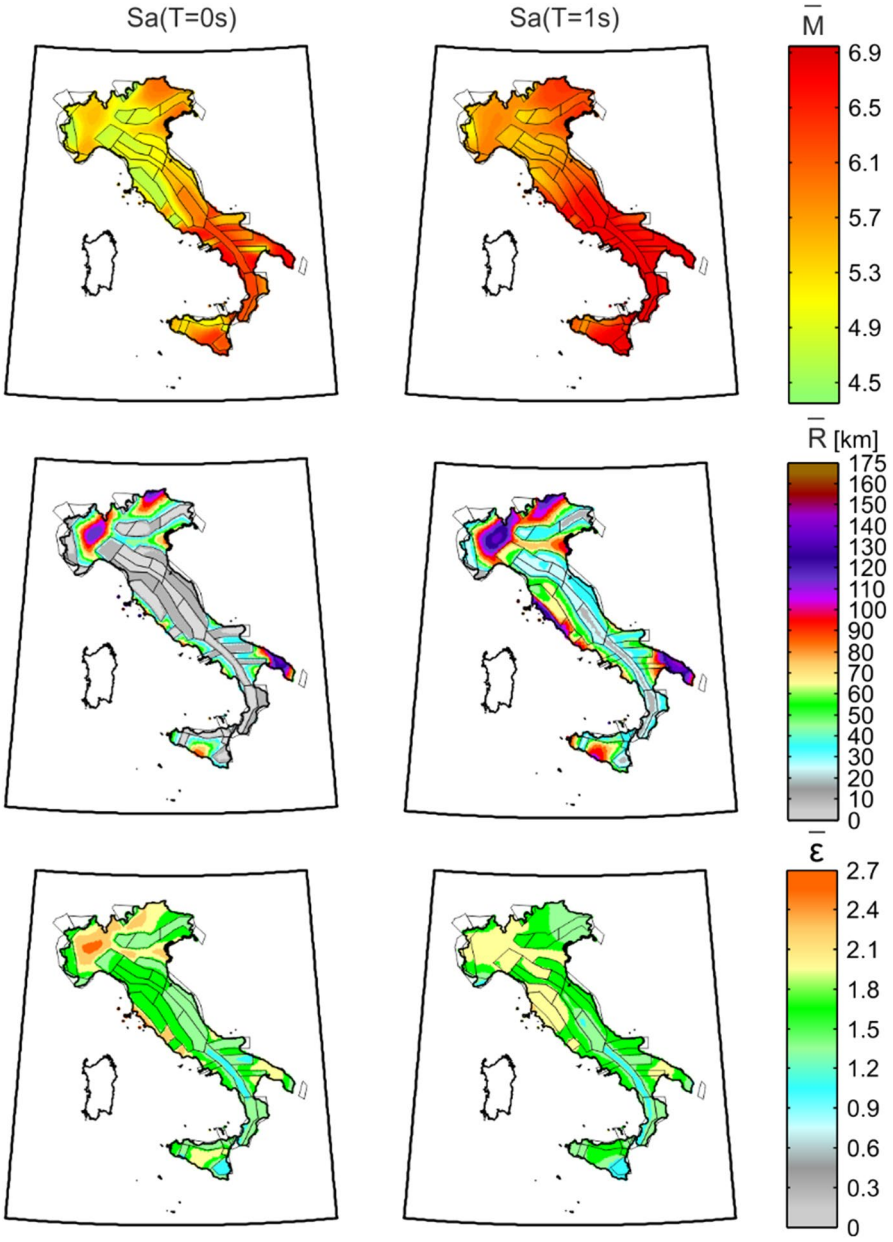

Fig. 3 Maps of $\{\overline{M}, \overline{R}, \overline{\varepsilon}\}$, that is mean magnitude, source-to-site distance and standardized residual of the ground-motion prediction equation, from hazard disaggregation for the exceedance of two ordinates of the 475 years UHS at each site (i.e., node of the computation grid). Left is PGA, right is $Sa(T = 1\ \text{s})$

distance from disaggregation is not small for sites outside any seismic source zone, given that close earthquakes cannot occur according to the considered source model, which does not have background seismicity. Finally, as it regards mean ε, it is generally

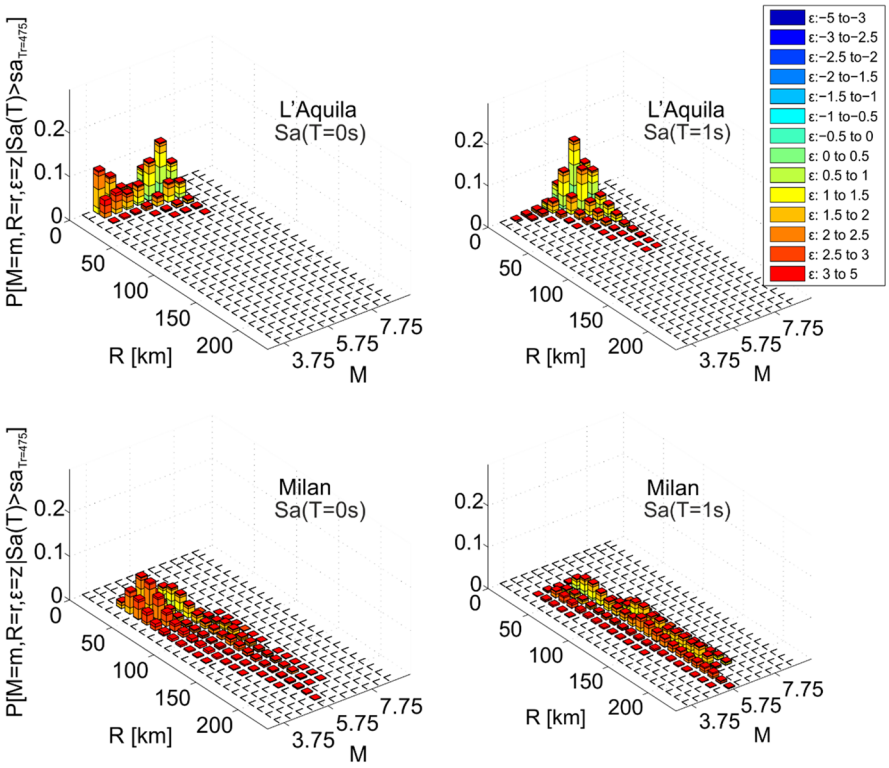

Fig. 4 Disaggregation distributions conditional to exceedance of $sa_{T_r=475}$ for L'Aquila (top) and Milan (bottom). Left is $Sa(T = 0$ s) and right is $Sa(T = 1$ s)

within one and two for sites within seismic source zones, while it can be larger outside the zones, meaning that in the lower hazard regions a significantly more "anomalous" ground-motion (i.e., away from the mean of the logarithms of IM, conditioned to a specific magnitude-distance pair, provided by the GMPE) is likely to cause exceedance of the 475 years UHS at the selected ordinates, with respect to sites within seismic source zones.

These considerations fully apply to L'Aquila and Milan. For the former site the mean vectors are $\{\overline{M} = 5.9, \overline{R} = 9$ km$, \overline{\varepsilon} = 1.4\}$ and $\{\overline{M} = 6.7, \overline{R} = 19$ km$, \overline{\varepsilon} = 1.2\}$ for $Sa(T = 0$ s) and $Sa(T = 1$ s), respectively. Whereas, for the latter, the mean vectors are $\{\overline{M} = 5.2, \overline{R} = 76$ km$, \overline{\varepsilon} = 2.2\}$ and $\{\overline{M} = 5.8, \overline{R} = 117$ km$, \overline{\varepsilon} = 2.0\}$ for $Sa(T = 0$ s) and $Sa(T = 1$ s), respectively.

In fact, because the full disaggregation distribution is needed for the purposes of this study (to follow), these are provided, for illustration, for the two sites in Fig. 4. These distributions were calculated replacing $\{dm, dr, dz\}$ with $\{\Delta m, \Delta r, \Delta z\}$ finite bins, which are wide: 0.05 magnitude units, 1 km for distance, and 0.05 ε units (i.e., the same bins used to compute hazard shown in Fig. 2) and allowed replacing $f_{M,R,\varepsilon|Sa(T)>sa}(m, r, z) \cdot dm \cdot dr \cdot dz$ with finite probabilities $P[M = m, R = r, \varepsilon = z|Sa(T) > sa_{T_r=475}]$, which are given in Fig. 4 (for representation purposes the bins in the figure are larger than actually computed).

For L'Aquila one notices that, with respect to source-to-site distance, the dominating contributions to exceedance of $sa_{T_r=475}$ are by close events, which means that the source zone where the site is enclosed into (Fig. 2), dominate the hazard; see Iervolino et al. (2011), for a discussion. As it regards the magnitude, the rate of exceedance of $Sa(T = 0\ \text{s})$ is contributed by different magnitudes, starting from relatively low values; when $Sa(T = 1\ \text{s})$ is of concern, larger magnitudes become more relevant in terms of probability of being causative of exceedance, as expected.

Looking at disaggregation for Milan, it emerges that contributions are more disperse among far earthquakes (above 30 km), which is the minimum distance from a source zone (also recalling that the source model considered in this study does not consider background seismicity). In fact, disaggregation distributions are contributed by two of the multiple sources that surround the site and affect its hazard.

3 The peak-over-the-threshold in Italy

Given the exceedance of the design spectral ordinates, it is worthwhile to assess which accelerations a structure is exposed to, which is the first result of this study. In fact, the expected value of $Sa(T)$ given the exceedance of $sa_{T_r=475}$ (i.e., the conditional mean) at the site is evaluated and mapped for Italy; it can be indicated as $E[Sa(T)|Sa(T) > sa_{T_r=475}]$. It is related to the action, expressed in terms of $Sa(T)$, a structure should withstand in strong earthquakes, that is, those able to cause exceedance of the design spectrum; thus, it can be a valuable piece of information.

The expected peak-over-the-threshold can be computed via Eq. (5), which derives from Eqs. (3) and (4); for convenience of the reader the full derivation of the equation is given in "Appendix".

$$E\left[Sa(T)\middle|Sa(T) > sa_{T_r=475}\right] = \iint_{M,R} e^{\mu_{m,r}} \cdot \int_{\frac{\log\left(sa_{T_r=475}\right)-\mu_{m,r}}{\sigma}}^{+\infty} e^{\sigma\cdot z} \cdot f_{M,R,\varepsilon|Sa(T)>sa_{T_r=475}}(m,r,z) \cdot dz \cdot dr \cdot dm \tag{5}$$

This expression, which only depends on the GMPE and on the disaggregation distribution, $f_{M,R,\varepsilon|Sa(T)>sa_{T_r=475}}(m,r,z)$, is exact in providing the mean of the random variable representing the spectral acceleration conditioned on the exceedance of $sa_{T_r=475}$. Nevertheless, it can be worthwhile to explain how the integrals in Eq. (5) are approximated when the disaggregation distribution is available in discrete form per $\{M, R, \varepsilon\}$ bins. This is discussed with reference to Fig. 4; in this case the probabilities $P[M = m, R = r, \varepsilon = z|Sa(T) > sa_{T_r=475}]$ are available and the computation of Eq. (5) proceeds as follows:

1. for any $\{M = m, R = r\}$ bin, the values of ε that are larger than $z^* = [\log(sa_{T_r=475}) - \mu_{m,r}]/\sigma$ are identified;
2. for each of the identified values, z, the probability $P[M = m, R = r, \varepsilon = z|Sa(T) > sa_{T_r=475}]$ is multiplied by $e^{\sigma\cdot z}$, where σ is the standard deviation of the GMPE as per Eq. (3);
3. the values obtained in the previous step are summed up obtaining a single value, that is: $\sum_{\varepsilon>z^*} e^{\sigma\cdot z} \cdot P[M = m, R = r, \varepsilon = z|Sa(T) > sa_{T_r=475}]$;

4. the obtained value, which corresponds to a specific $\{M = m, R = r\}$ bin, is then multiplied by $e^{\mu_{m,r}}$, that is: $e^{\mu_{m,r}} \cdot \sum_{\varepsilon > z^*} e^{\sigma \cdot z} \cdot P[M = m, R = r, \varepsilon = z | Sa(T) > sa_{T_r=475}]$;
5. steps 1–4 are repeated for all $\{M, R\}$ bins (i.e., all those in Fig. 4) and the results summed up obtaining a single value, that is the expected value of acceleration given exceedance: $E[Sa(T)|Sa(T) > sa_{T_r=475}] = \sum_M \sum_R e^{\mu_{m,r}} \cdot \sum_{\varepsilon > z^*} e^{\sigma \cdot z} \cdot P[M = m, R = r, \varepsilon = z | Sa(T) > sa_{T_r=475}]$. In fact, this latter equation is the sought approximation of Eq. (5).

Finally note that this procedure, although illustrated for $sa_{T_r=475}$, can be applied to compute the expected value of acceleration given the exceedance of any arbitrarily defined threshold. Moreover, in the case of hazard computed by means of a logic tree, the expected value in Eq. (5) can be computed branch-by-branch and then the results weighted consistent with the logic tree assumptions.

3.1 Peak-over-the-threshold maps

The map of $E[Sa(T)|Sa(T) > sa_{T_r=475}]$ given in Fig. 5, was obtained from the disaggregation distributions calculated for the nodes of the same grid used to compute the hazard map given in Fig. 2.

Figure 5 (top) provides the expected accelerations given the exceedance of PGA (left) and $Sa(T = 1\text{ s})$ (right) that have 475 years return period of exceedance at each site (Fig. 2). The middle panels show the absolute difference between the peak and the threshold: $\Delta = E[Sa(T)|Sa(T) > sa_{T_r=475}] - sa_{T_r=475}$. Finally, the bottom panels show the difference in percentage terms: $\Delta^{\%} = 100 \cdot \{E[Sa(T)|Sa(T) > sa_{T_r=475}] - sa_{T_r=475}\}/sa_{T_r=475}$.

The figure shows that, in the case of exceedance of $sa_{T_r=475}$, one should expect the largest excursion above the design spectrum in those locations where the hazard is larger (i.e., at the sites where the exceeded threshold is larger). Most importantly, for $Sa(T = 1\text{ s})$, such expected exceedance can be as high as 0.51 g in absolute terms (occurring within zone 929) and more than 150% in terms of percentage difference (occurring within zone 935). This means that accelerations that are up to 2.5 times the threshold should be expected in case of exceedance. In other words, a structure is expected to be subjected to an acceleration more than twice the one considered by design.

The percentage difference varies significantly from site-to-site across the country, even if the threshold has a fixed return period. Its average over the country is 70% for $Sa(T = 1\text{ s})$ and 50% for PGA. The minimum percentage difference of $E[Sa(T = 1\text{ s})|Sa(T = 1\text{ s}) > sa_{T_r=475}]$ occurs in the lowest hazard regions, that is, outside any source zone (close to Turin in northern Italy) and is around 45%, meaning that in these areas the expected accelerations, in case of exceedance, are about 1.5 times the design value. It is also to note that while the largest accelerations are expected for PGA, the largest excursions over the spectrum are expected for $Sa(T = 1\text{ s})$.

It is worthwhile now to compare Fig. 5 with the disaggregation maps in Fig. 3 (bottom panels). It is worth noting that the peak-over-the-threshold is smaller at sites where the hazard is lower. Conversely, at these sites, ε tends to assume larger values. For example, in Milan the mean of ε from disaggregation is around 2 for both PGA and $Sa(T = 1\text{ s})$, while in L'Aquila it is between 1.2 and 1.4 for both spectral ordinates. Conversely, looking

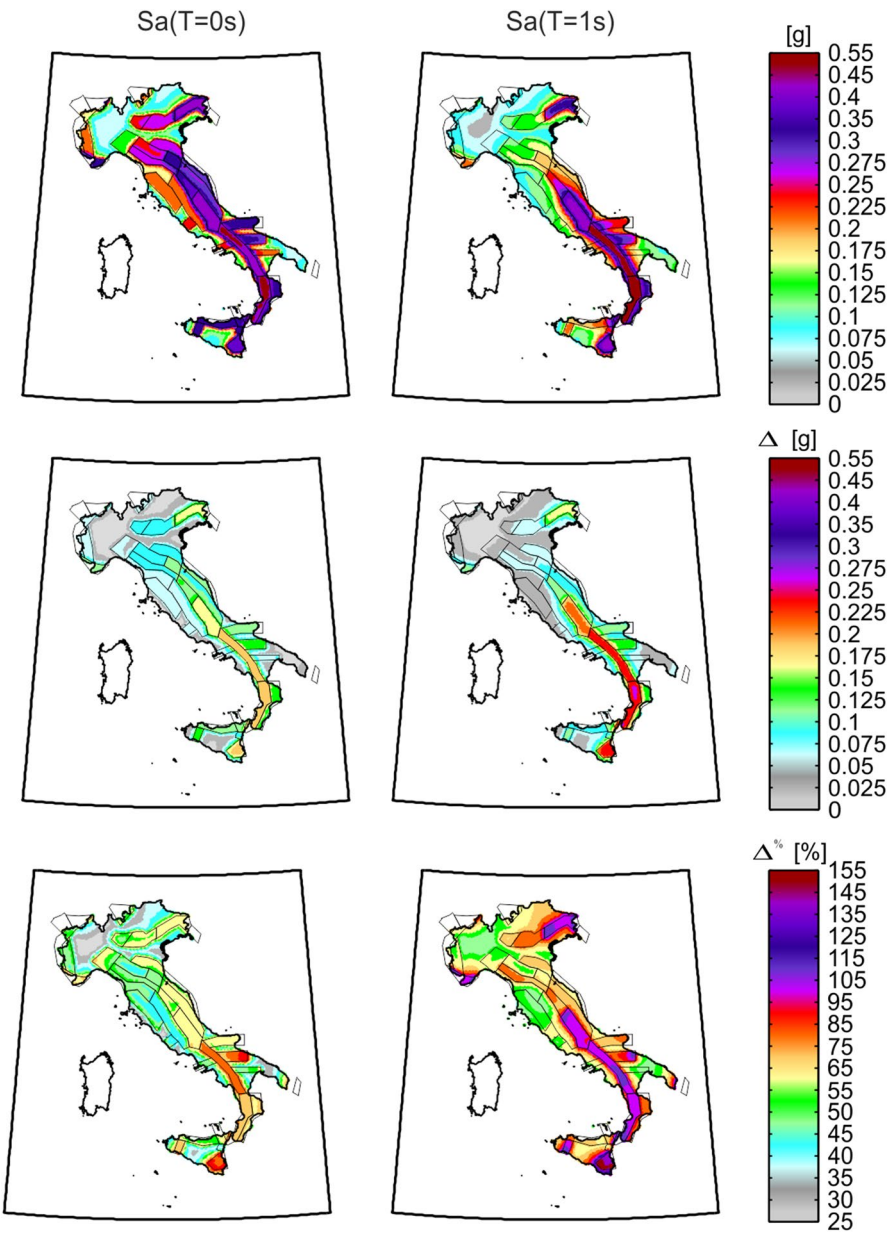

Fig. 5 Map of the expected value of acceleration given the exceedance of two ordinates of the 475 years UHS at each site (i.e., node of the computation grid) in Italy. Top is the expected value of the acceleration given exceedance; middle is the difference between the expected acceleration and the exceeded threshold; bottom is the percentage exceedance

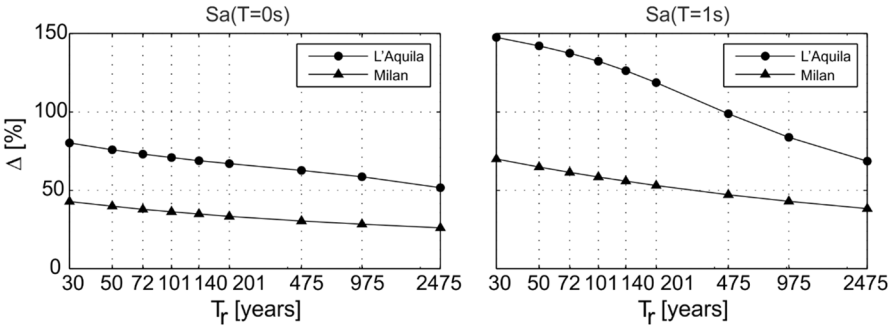

Fig. 6 Percentage exceedance of two ordinates of UHS in L'Aquila and Milan, as a function of the return period of the acceleration being exceeded

at Fig. 5, it emerges that the peak-over-the-threshold increase in Milan is, in percentage terms, less than half than in L'Aquila.[5]

3.2 Peak-over-the-threshold as a function of local soil conditions

It is to remark that, although the maps in the top panels of Fig. 5 are developed for rock, the conditional mean of exceedance for another site class, characterized by a specific θ -value in Eq. (3), can be simply obtained as $e^{\theta} \cdot E[Sa(T)|Sa(T) > sa_{T_r=475}]$; this is shown in "Appendix" and follows from what discussed in Iervolino (2016). Therefore, the absolute differences for rock should be also scaled by e^{θ}, while percentage differences are soil-independent. For the considered GMPE of Ambraseys et al. (1996), the e^{θ} values for *stiff soil* are equal to 1.31 and 1.34 for PGA and $Sa(T = 1\text{s})$, respectively. For *soft soil* they are equal to 1.33 and 1.66 for PGA and $Sa(T = 1\text{s})$, respectively. The reader can, therefore, easily modify the values in the maps according to arbitrary soil site classes. (Note that this shortcut only applies for GMPEs of the type in Eq. (3), which could not be the case for several recent models; see Douglas 2014).

3.3 Peak-over-the-threshold as a function of the design return period

The results discussed so far refer to $T_r = 475$ years, while it is worthwhile to see the effect of the return period on the peak-over-the-threshold. To this aim the cases of L'Aquila and Milan are analyzed in Fig. 6. In the figure, the percentage increment, the same as in Fig. 5 (bottom), are given for the spectral ordinates thresholds corresponding to the nine return periods the Italian code refers to for design; i.e., 30, 50, 72, 101, 140, 201, 475, 975 and 2475 years. The spectral ordinates associated with each return period were calculated via the same source model and procedure described above.

[5] These maps are consistent with the hazard model used to derive the $sa_{T_r=475}$ thresholds with respect to which the expected value of acceleration given exceedance is evaluated; therefore, at the same time, they inherently reflect its features. Nevertheless, the procedure discussed in Sect. 3 and demonstrated in "Appendix" is general and can be applied to any hazard model.

The curves generally indicate that the expected exceedance decreases mildly for $T_r \geq 200$ years. For the PGA, the expected exceedance is never smaller than 1.5 times the threshold for L'Aquila and 1.3 for Milan. Percentage differences are larger for $Sa(T = 1\text{ s})$ than $Sa(T = 0\text{ s})$ and the minimum value, in the investigated range of return periods, is 1.7 and 1.4 times the exceeded threshold for L'Aquila and Milan, respectively. This means that, in case of exceedance, the expected peak is significantly above the spectrum, even if the largest return period (i.e., 2475 years) is considered for design. As discussed, all these values of percentage differences, are soil-independent.

4 Conclusions

Seismic codes at the state-of-the-art take advantage of PSHA via uniform hazard spectra, the return period of exceedance of which is determined based on the structural performance of interest. It has been discussed in the literature and it is trivial to show, that the UHS' are such that they are likely-to-very-likely going to be exceeded in the epicentral areas of earthquakes with magnitudes that can be considered relatively moderate (i.e., with relatively large frequency of occurrence over the country). The consequence of interest to structural engineering is that in the epicentral area of these events the seismic actions the structure must withstand are likely beyond those determined for design, and it might be useful to quantify them.

The simple study presented herein aimed, with reference to Italy where design spectra are close approximations of UHS', at quantifying elastic seismic actions structures are subjected to in the case of strong earthquakes; i.e., those able to exceed the code spectrum. Nationwide maps were developed in the presented study in a consistent manner with respect to the same model used to define elastic seismic actions according to the current Italian code, and mostly refer to 475 years exceedance return period of the design action. Moreover, in two specific sites, in high- and low-hazard regions, the effects of the return period of exceedance of the UHS, in a range of interest to the code, were evaluated. The following was found.

- Exceedance is expected to be up to 2.5 times the design spectrum and occurs in the most hazardous sites. In the less hazardous regions (i.e., outside the seismic source zones), the expected value above the UHS is smaller in relative terms (e.g., 1.5 times).
- Disaggregation shows that the expected value of ε from disaggregation is larger for less hazardous sites with respect to high hazard regions, meaning that in the former case exceedance is likely due to a more "anomalous" ground-motion with respect to the latter. Based on this same argument, it also results that, even if in the most hazardous regions exceedance is expected from more ordinary ground-motions (lower ε), the expected exceedance is larger.
- Expected accelerations given exceedance are larger for the lower natural vibrations periods; on the other hand, excursions over the design elastic threshold are larger for $Sa(T = 1\text{ s})$ than PGA, indicating a larger exposure to exceedance at lower natural vibration periods.
- The peak-over-the-threshold is amplified by soil conditions, in absolute terms, by a factor that only depends on the considered ground-motion prediction equation, while the percent difference is soil-invariant. (This applies because of the classical structure of the GMPEs to compute design actions in Italy.)

The study of L'Aquila and Milan sites, allowed evaluating the trend of the peak-over-the-threshold as a function of the return period of exceedance of the design spectrum. It is found that, for the most hazardous regions, the expected elastic acceleration a structure should withstand in the case of exceedance of the elastic actions never goes below 1.5 times the threshold. It is also found that, even designing for the largest return period the code allows, the expected amount of exceedance is between 30% and 70% of the considered spectrum.

These results can be helpful in quantifying what to expect for code-conforming structures in countries where probabilistic seismic hazard lies at the basis of structural design and/or for more informed performance-based seismic design aimed at controlling the structural performance in epicentral areas of strong earthquakes. In fact, in these areas structural safety is most required, yet it is likely that the seismic elastic actions go beyond the design ones.

Acknowledgements This article was developed within the activities of the ReLUIS-DPC 2014–2018 research project, funded by *Presidenza del Consiglio dei Ministri – Dipartimento della Protezione Civile*. The conclusions and opinions expressed, does not necessarily correspond to those of the funding entity. The helpful comments by Simone Barani (*Università degli Studi di Genova*) and Laurentiu Danciu (*Swiss Seismological Service*) are also acknowledged.

Appendix

The expected value (e.g., Mood et al. 1974) of the random variable representing the spectral acceleration given exceedance (i.e., the conditional mean) can be computed applying the *law of total expectation*, with respect to $\{M, R, \varepsilon\}$:

$$E\left[Sa(T)\middle|Sa(T) > sa_{T_r=475}\right] = \iiint_{M,R,\varepsilon} E\left[Sa(T)\middle|Sa(T) > sa_{T_r=475}, M = m, R = r, \varepsilon = z\right] \cdot f_{M,R,\varepsilon\,|Sa(T)>sa_{T_r=475}}(m, r, z) \cdot dz \cdot dr \cdot dm, \tag{6}$$

where, $E\left[Sa(T)\middle|Sa(T) > sa_{T_r=475}, M = m, R = r, \varepsilon = z\right]$ is the expected value of acceleration given exceedance and $\{M, R, \varepsilon\}$, while, as already discussed $f_{M,R,\varepsilon\,|Sa(T)>sa_{T_r=475}}$ is from hazard disaggregation. Now considering that, according to Eq. (3) and assuming $\theta = 0$ to identify rock soil conditions, it is $E\left[Sa(T)\middle|Sa(T) > sa_{T_r=475}, M = m, R = r, \varepsilon = z\right] = e^{\mu_{m,r}+\sigma\cdot z}$, then:

$$E\left[Sa(T)\middle|Sa(T) > sa_{T_r=475}\right] = \iiint_{M,R,\varepsilon} e^{\mu_{m,r}+\sigma\cdot z} \cdot f_{M,R,\varepsilon\,|Sa(T)>sa_{T_r=475}}(m, r, z) \cdot dz \cdot dr \cdot dm, \tag{7}$$

at this point, recognizing that $e^{\mu_{m,r}}$ does not depend on ε and that $Sa(T) > sa_{T_r=475}$ implies $\varepsilon > \left[\log\left(sa_{T_r=475}\right) - \mu_{m,r}\right]/\sigma$, one gests the result in Eq. (8), which coincides with Eq. (5):

$$E\left[Sa(T)\middle|Sa(T) > sa_{T_r=475}\right] = \iint_{M,R} e^{\mu_{m,r}} \cdot \int_{\frac{\log\left(sa_{T_r=475}\right)-\mu_{m,r}}{\sigma}}^{+\infty} e^{\sigma\cdot z} \cdot f_{M,R,\varepsilon\,|Sa(T)>sa_{T_r=475}}(m, r, z) \cdot dz \cdot dr \cdot dm. \tag{8}$$

If now one wants to compute the expected peak-over the threshold for a soil conditions different from rock, say $E\left[Sa(T)\middle|Sa(T) > sa_{T_r=475}, \theta\right]$, it is sufficient to amplify the value obtained for rock by e^{θ}, where θ is the coefficient of Eq. (3) for the soil class of interest. This is because replacing $e^{\mu_{m,r}+\sigma\cdot e+\theta}$ in Eq. (7) and recognizing that θ does not depend on $\{M, R, \varepsilon\}$, it results:

$$E\left[Sa(T)\middle|Sa(T) > sa_{T_r=475}, \theta\right] = e^{\theta} \cdot \iint_{M,R} e^{\mu_{m,r}} \cdot \int_{\frac{\log\left(sa_{T_r=475}\right)-\mu_{m,r}}{\sigma}}^{+\infty} e^{\sigma\cdot z} \cdot f_{M,R,\varepsilon\left|Sa(T)>sa_{T_r=475}\right.}(m, r, z)\cdot dz \cdot dr \cdot dm = e^{\theta} \cdot E\left[Sa(T)\middle|Sa(T) > sa_{T_r=475}\right]. \quad (9)$$

As discussed in the body of the text, clearly this shortcut applies only for GMPEs of the type in Eq. (3).

References

Ambraseys NN, Simpson KA, Bommer JJ (1996) Prediction of horizontal response spectra in Europe. Earthq Eng Struct D 25:371–400

Barani S, Spallarossa D, Bazzurro P (2009) Disaggregation of probabilistic ground-motion hazard in Italy. Bull Seismol Soc Am 99:2638–2661

Barani S, Albarello D, Spallarossa D, Massa M (2017a) Empirical scoring of ground-motion prediction equations for probabilistic seismic hazard analysis in Italy including site effects. Bull Earthq Eng 15:2547–2570

Barani S, Albarello D, Massa M, Spallarossa D (2017b) Influence of twenty years of research on ground-motion prediction equations on probabilistic seismic hazard in Italy. Bull Seismol Soc Am 107:240–255

Bazzurro P, Cornell CA (1999) Disaggregation of seismic hazard. Bull Seismol Soc Am 89:501–520

Bommer JJ, Douglas J, Strasser FO (2003) Style-of-faulting in ground-motion prediction equations. Bull Earthq Eng 1:171–203

CEN (2004) European Committee for Standardisation. Eurocode 8: design provisions for earthquake resistance of structures, part 1.1: general rules, seismic actions and rules for buildings, prEN 1998-1

Chioccarelli E, De Luca F, Iervolino I (2012) Preliminary study of Emilia (May 20th 2012) earthquake ground-motion records V2.11. Available at http://www.reluis.it/. Accessed Apr 2018

CSLLPP (2008) Decreto Ministeriale 14 gennaio 2008: Norme tecniche per le costruzioni, no. 29. Gazzetta Ufficiale della Repubblica Italiana **(in Italian)**

Douglas J (2014) Fifty years of ground-motion models. In: 2ECEES 2nd European conference on earthquake engineering and seismology, Istanbul, Turkey

Iervolino I (2013) Probabilities and fallacies: why hazard maps cannot be validated by individual earthquakes. Earthq Spectra 29:125–1136

Iervolino I (2016) Soil-invariant seismic hazard and disaggregation. Bull Seismol Soc Am 106:1900–1907

Iervolino I, Giorgio M (2017) È possibile evitare il superamento delle azioni di progetto nell'area epicentrale di terremoti forti? Progett Sismica 8:25–32 **(in Italian)**

Iervolino I, Chioccarelli E, Convertito V (2011) Engineering design earthquakes from multimodal hazard disaggregation. Soil Dyn Earthq Eng 31:1212–1231

Iervolino I, Chioccarelli E, Cito P (2016) REASSESS V1.0: a computationally-efficient software for probabilistic seismic hazard analysis. In: VII ECCOMAS European Congress on Computational Methods in Applied Sciences and Engineering, Crete Island, Greece

Iervolino I, Baltzopoulos G, Chioccarelli E, Suzuki A (2017a) Seismic actions on structures in the near-source region of the 2016 central Italy sequence. Bull Earthq Eng. https://doi.org/10.1007/s10518-017-0295-3

Iervolino I, Spillatura A, Bazzurro P (2017b) RINTC Project—assessing the (implicit) seismic risk of code-conforming structures in Italy. In: COMPDYN, VI ECCOMAS thematic conference on computational methods in structural dynamics and earthquake engineering, Rhodes Island, Greece

Iervolino I, Chioccarelli E, Cito P (2018) Which earthquakes are expected to exceed the design spectra? **(in review)**

Joyner WB, Boore DM (1981) Peak horizontal acceleration and velocity from strongmotion records including records from the 1979 Imperial Valley, California, Earthquake. Bull Seismol Soc Am 71:2011–2038

Masi A, Chiauzzi L, Braga F, Mucciarelli M, Vona M, Ditommaso R (2011) Peak and integral seismic parameters of L'Aquila 2009 ground-motions: observed versus code provision values. Bull Earthq Eng 9:139–156

McGuire RK (2004) Seismic hazard and risk analysis. Report MNO-10. Earthquake Engineering Research Institute Oakland

Meletti C, Galadini F, Valensise G, Stucchi M, Basili R, Barba S, Vannucci G, Boschi E (2008) A seismic source zone model for the seismic hazard assessment of the Italian territory. Tectonophysics 450(1):85–108

Montaldo V, Faccioli E, Zonno G, Akinci A, Malagnini L (2005) Treatment of ground-motion predictive relationships for the reference seismic hazard map of Italy. J Seismol 9:295–316

Mood AM, Graybill FA, Boes D (1974) Introduction to the theory of statistics. McGraw-Hill, New York

Stucchi M, Meletti C, Montaldo V, Crowley H, Calvi GM, Boschi E (2011) Seismic hazard assessment (2003–2009) for the Italian Building Code. Bull Seismol Soc Am 101:1885–1911